nature microbiology

ARTICLES

DOI: 10.1038/s41564-017-0037-y

Contribution of reactive oxygen species to thymineless death in *Escherichia coli*

Yuzhi Hong[1], Liping Li[1], Gan Luan[1], Karl Drlica[1] and Xilin Zhao[1,2*]

Nutrient starvation usually halts cell growth rather than causing death. Thymine starvation is exceptional, because it kills cells rapidly. This phenomenon, called thymineless death (TLD), underlies the action of several antibacterial, antimalarial, anticancer, and immunomodulatory agents. Many explanations for TLD have been advanced, with recent efforts focused on recombination proteins and replication origin (*oriC*) degradation. Because current proposals account for only part of TLD and because reactive oxygen species (ROS) are implicated in bacterial death due to other forms of harsh stress, we investigated the possible involvement of ROS in TLD. Here, we show that thymine starvation leads to accumulation of both single-stranded DNA regions and intracellular ROS, and interference with either event protects bacteria from double-stranded DNA breakage and TLD. Elevated levels of single-stranded DNA were necessary but insufficient for TLD, whereas reduction of ROS to background levels largely abolished TLD. We conclude that ROS contribute to TLD by converting single-stranded DNA lesions into double-stranded DNA breaks. Participation of ROS in the terminal phases of TLD provides a specific example of how ROS contribute to stress-mediated bacterial self-destruction.

When cells are starved of nutrients (amino acids, nucleotides, or vitamins), growth usually stops until the nutrient becomes available[1]. Starvation of thymine or thymidine (T-starvation) is different, and cells die rapidly[2,3]. Both prokaryotic and eukaryotic cells exhibit this phenomenon, known as thymineless death (TLD)[1]. The mechanism of TLD is of considerable interest, because it underlies the effectiveness of several antibacterial (trimethoprim, sulfamethoxazole), antimalarial (pyrimethamine, sulfonamide), anticancer (methotrexate, fluorouracil), and immune-modulating (methotrexate) agents. Proposed explanations for TLD have included unbalanced growth[2], toxin-antitoxin module action[4], nucleotide misincorporation[5], induction of the SOS regulon[6], and destruction of replication forks[7–9]. Previous work has also focused on recombination events, some of which are protective and some of which are destructive[6,9–11]. Recent studies suggested that TLD in *Escherichia coli* derives from the degradation of the replication origin (*oriC*)[6,12–15]. However, the *oriC* copy number, relative to that of the replication terminus, fails to drop below unity[6,12,14], indicating an incomplete loss of *oriC*. The remaining *oriC* should be sufficient for viability when thymine becomes available for recombinational repair. Moreover, a counter-example occurs with a *thyA-recBC* double mutant in which preferential loss of *oriC* is eliminated, but death due to T-starvation is not[14]. Overall, previous work does not explain why genetic perturbations only partially block the death process; moreover, some explanations are weakened by counter-arguments[1,16–18]. Thus, additional work is needed to understand the events involved in TLD.

Among the unexplained observations is a reduction in TLD by deficiencies in the recombination genes *recQ* and *recF*[6,11,19,20]. The wild-type products may be destructive during T-starvation by increasing single-stranded DNA (ssDNA) regions[7,21]. Because double-stranded DNA breaks (DSBs) are involved in TLD[9,14,22], ssDNA regions/lesions, enlarged by RecF and RecQ, may serve as substrates for DNA breakage as part of a self-destructive response to stress. Work with antimicrobials indicates that some destructive stress responses involve reactive oxygen species (ROS)[23–26]; in the case of TLD, persistent ssDNA regions/lesions[14] may be substrates for the production of lethal DSBs by ROS.

The present work used three strategies to examine the role of ROS in TLD. One interfered with ROS accumulation by inhibiting hydroxyl radical production/accumulation using chemical inhibitors. A second examined the effects of mutations in genes that normally influence ROS levels or the accumulation of ssDNA regions. The third approach used flow cytometry to monitor ROS and fluorescence microscopy to measure the prevalence of *E. coli* cells containing elevated ROS levels, ssDNA regions and DSBs, each of which accumulated during T-starvation of cells grown in a defined, nutrient-rich medium. ssDNA regions/lesions were necessary but insufficient for TLD, an observation that was consistent with their conversion into lethal DSBs by ROS.

Results

ROS are associated with TLD. To monitor ROS levels, we examined the fluorescence of ROS-sensitive dyes. Removal of thymidine from cultures of an *E. coli* thymidylate synthetase mutant (*ΔthyA*) increased intracellular ROS, as monitored by flow cytometry (Fig. 1a) and by fluorescence microscopy (Supplementary Fig. 1a) using carboxy-H2DCFDA, a fluorescent ROS indicator dye. The surge in intracellular ROS paralleled cell death (compare Fig. 1a,b and Supplementary Fig. 1b). Moreover, a dye specific for hydrogen peroxide, Peroxy Orange-1, revealed the accumulation of H_2O_2 during TLD (Fig. 1c and Supplementary Fig. 1c). T-starvation also increased lipid peroxidation, as indicated by fluorescence of C11-BODIPY, a dye specific for lipid peroxidation (Fig. 1d and Supplementary Fig. 1d). Control experiments showed very low ROS accumulation by either wild-type cells growing without thymidine or by the *ΔthyA* mutant growing in medium containing thymidine (Supplementary Fig. 1e–h). Moreover, autofluorescence contributed little to our measurements, as cells with no dye showed no background fluorescence during microscopy and a

[1]Public Health Research Institute and Department of Microbiology, Biochemistry & Molecular Genetics, New Jersey Medical School, Rutgers University, 225 Warren Street, Newark, NJ 07103, USA. [2]State Key Laboratory of Molecular Vaccinology and Molecular Diagnostics, School of Public Health, Xiamen University, South Xiang-An Road, Xiang-An District, Xiamen, Fujian Province 361102, China. *e-mail: zhaox5@njms.rutgers.edu

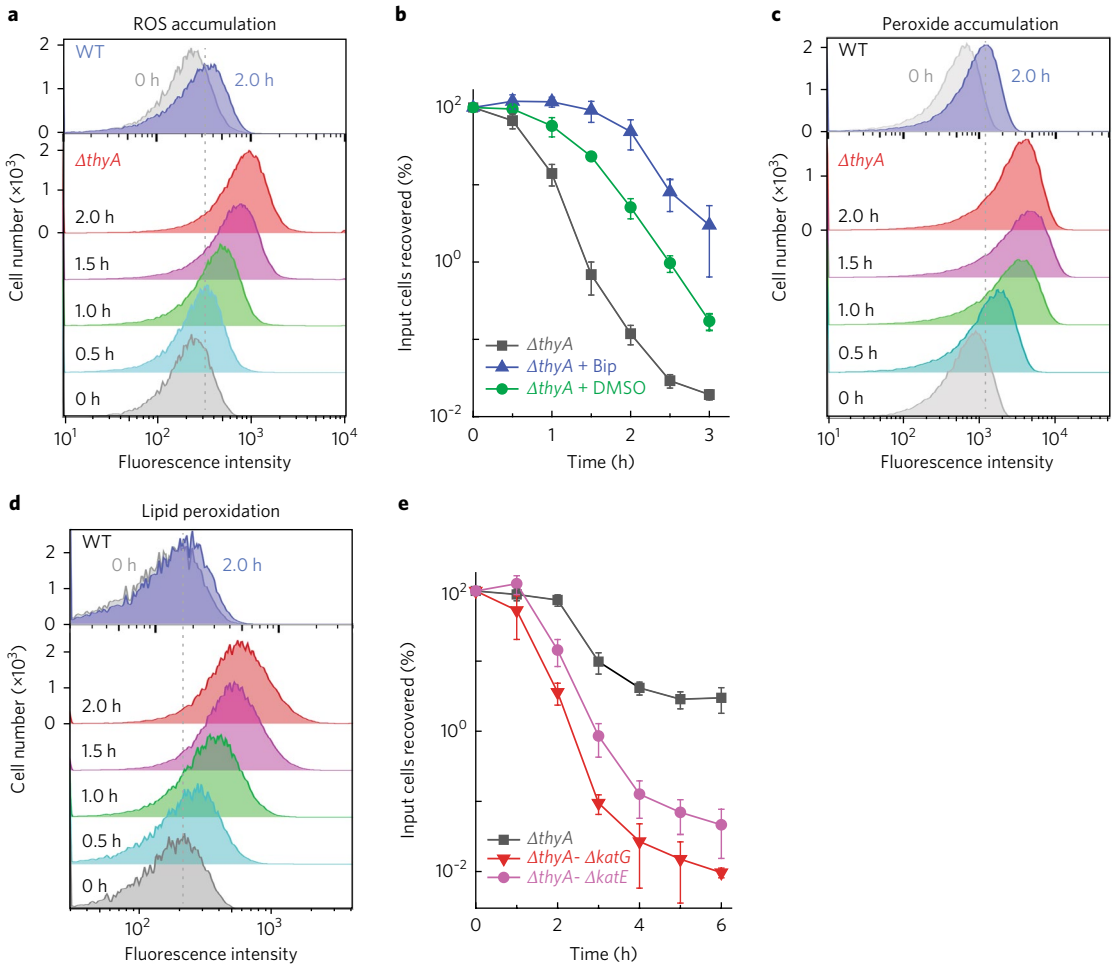

Fig. 1 | Association of ROS with TLD. a, ROS accumulation in a *ΔthyA* mutant (strain 3640). T-starvation extended for the indicated times. ROS accumulation was monitored by flow cytometry using carboxy-H2DCFDA-mediated fluorescence. **b**, Inhibition of TLD. Rapid death of a thymidine-starved *ΔthyA* culture (squares) was reduced by 2,2′-bipyridyl (Bip, triangles) or dimethyl sulfoxide (DMSO, circles), each at 0.5 × MIC. Bipyridyl at 0.5 × MIC slightly suppressed growth, but such growth inhibitory effects cannot account for the large protection from TLD (see Supplementary Fig. 14 for details). **c**, H_2O_2 accumulation during TLD. H_2O_2 was monitored at the indicated times after initiation of T-starvation by flow cytometry using Peroxy Orange-1-mediated fluorescence. **d**, Lipid peroxidation during TLD. Lipid peroxidation at the indicated times was detected by flow cytometry using C11-BODIPY-mediated fluorescence. **e**, Exacerbation of TLD by catalase/peroxidase deficiencies. Deletion of *katG* (strain 3641) or *katE* (strain 3645), when present with a *ΔthyA* mutation, decreased cell survival for samples taken at the indicated times during T-starvation. A nutrient-rich, defined medium (Hi-DEF Azure) was used for **a**–**d**. M9 minimal medium was used for **e** (see Supplementary Fig. 3d for KatG/E effects in Hi-DEF Azure medium). Plots in **a**, **c** and **d** are representative of three independent experiments. Data points are averages of three independent experiments in **b** and **e**. Error bars represent standard deviation of the mean.

much lower fluorescence intensity upshift in flow cytometry than when dye was present (Supplementary Fig. 2). Thus, an increase in ROS accompanies TLD.

We next perturbed the ROS levels. Agents that inhibit ROS accumulation, such as the iron chelator 2,2′-bipyridyl[23,27] or the hydroxyl-radical scavenger dimethyl sulfoxide (DMSO)[28], reduced both ROS accumulation and TLD (Fig. 1b and Supplementary Fig. 3a–c). Conversely, deletion of peroxide-detoxifying genes, such as *katG*/*E*, generated a hyperlethal phenotype during T-starvation (Fig. 1e and Supplementary Figs. 3d and 4a). We performed the latter experiment with minimal medium, because the higher ROS levels in rich medium (Supplementary Fig. 3e–h) would mask the added effect of a catalase deficiency (Supplementary Fig. 3d). Two additional experiments supported involvement of ROS in TLD. First, when trimethoprim triggered TLD, lethal action was reduced by DMSO and exacerbated by a deficiency in *katG* (Supplementary Fig. 4a). Second, when a *ΔthyA* mutant growing anaerobically was starved for thymidine, TLD was lowered, and it was eliminated by additional treatment with bipyridyl (Supplementary Fig. 4b). Thus, TLD is associated with a surge in ROS, reduced by agents that inhibit ROS accumulation, and enhanced by deficiencies in genes that protect from ROS.

Respiratory genes are involved in ROS accumulation and TLD. General inhibitors of RNA and protein synthesis (rifampicin and chloramphenicol) abolish TLD[13,29,30], but the underlying mechanism is poorly understood due to the pleiotropic effects of these agents. Because both drugs reduce cellular respiration[31], and because ROS are normal byproducts of respiration, we expected these inhibitors to block TLD in part by suppressing ROS accumulation. Indeed, the surge in ROS associated with T-starvation was reduced by rifampicin and chloramphenicol (Fig. 2a,b).

We also asked whether particular respiratory proteins participate in ROS accumulation and TLD. In *E. coli*, ubiquinone transfers electrons from multiple input dehydrogenases to three output terminal oxidases (cytochromes *bd-I*, *bd-II* and *bo*[32]). Deletion of *ubiG*, a gene required for ubiquinone biosynthesis, decreased ROS accumulation and enhanced survival during T-starvation (Fig. 2c,d). Inactivation of *bd-I* oxidase

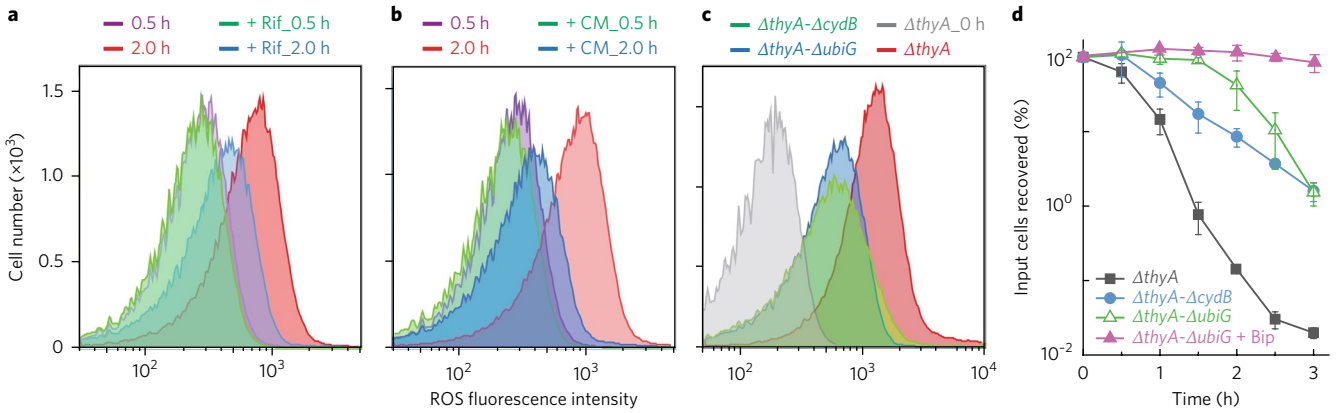

Fig. 2 | Suppression of ROS accumulation during T-starvation by rifampicin, chloramphenicol or deficiencies in respiratory-chain genes. ROS were measured by flow cytometry as in Fig. 1a unless otherwise stated. Colour coding for samples is shown above each panel. **a**, Effect of rifampicin. A *ΔthyA E. coli* strain (3640) was treated without or with 50 μg ml^{-1} rifampicin (+ Rif) when T-starvation was initiated. Samples were removed for flow cytometry at the indicated times. **b**, Effect of chloramphenicol. The method used was as in **a**, but with 40 μg ml^{-1} chloramphenicol (+ CM) instead of rifampicin. **c**, Effect of mutations in respiratory-chain genes on ROS. Cells were starved of thymidine for 3 h before samples were taken for flow cytometry. Bacterial strains were *ΔthyA-ΔubiG* (3812), *ΔthyA-ΔcydB* (4012), and *ΔthyA* (3640). **d**, Effect of mutations in respiratory-chain genes and bipyridyl on TLD. Cultures of double-deletion mutants (*ΔthyA-ΔubiG*, *ΔthyA-ΔcydB*) and *ΔthyA-ΔubiG* plus bipyridyl (0.5 × MIC) were starved of thymidine; per cent survival was determined at the indicated times. Plots in **a**–**c** are representative of three independent experiments. Data points in **d** are averages for three independent experiments, with error bars representing standard deviation of the mean.
No growth defect occurred when deficiencies in *cydB* and *thyA* were combined (Supplementary Fig. 14). A small inhibitory effect was observed with a *ΔthyA-ΔubiG* double mutant and with addition of bipyridyl to a *ΔthyA* mutant culture (Supplementary Fig. 14). However, substantial TLD was observed after a greater slowing of growth by incubation of the *ΔthyA* single mutant at 30 °C (Supplementary Fig. 14), thereby arguing against the small growth inhibition by *ΔubiG* or bipyridyl being a major reason for protection from TLD.

(*ΔcydB*) also reduced ROS accumulation and TLD (Fig. 2c,d). To attribute the reduction in TLD to deficiencies in *ubiG* and *cydB*, we showed that plasmid-borne copies of the wild-type genes restored *ΔthyA*-mediated TLD (Supplementary Fig. 5a,b). Disruption of the other terminal oxidases, AppBC (*bd-II* oxidase) or CyoABCDE (*bo* oxidase), or several of the many electron-input enzymes (succinate dehydrogenase or NADH dehydrogenases I or II), individually had no effect on either ROS accumulation or TLD (Supplementary Fig. 5c–f). Thus, *bd-1* oxidase is the major terminal oxidase responsible for the correlation of ROS production with TLD. These data fit with respiratory proteins contributing to TLD and support ROS involvement in TLD.

Because a deficiency of *ubiG* or *cydB* only partially eliminated the ROS surge or TLD, we next added bipyridyl to the *ΔthyA-ΔubiG* culture to further reduce ROS. This treatment reduced ROS to background levels and largely abolished TLD, even after prolonged (5 h) T-starvation (Fig. 2d and Supplementary Fig. 6a,b). Thus, ROS are the dominant source of TLD. The contribution of other cellular activities, such as replication, transcription and toxic recombination/repair, to TLD is probably through ROS-mediated events, because each is expected to persist in bipyridyl-treated *ΔthyA-ΔubiG* cultures in which neither ROS accumulation nor TLD occurs.

Accumulation of single-stranded DNA is necessary but insufficient for TLD. During TLD, bacterial chromosomes are expected to accumulate regions of ssDNA in lagging strands of replication forks and at sites of single-stranded lesion repair. Indeed, ssDNA lesions are observed during thymine starvation[22]. Due to the absence of deoxythymidine triphosphate (dTTP), these ssDNA regions/lesions cannot be filled and will tend to persist[14]. The role of ssDNA regions in TLD can be studied using deficiencies in RecQ and RecFOR recombinational repair, because these proteins are thought to generate/expand ssDNA regions[7,21,33]; moreover, deficiencies in *recQ* and *recF* protect from TLD[11,19,20]. Deletion of *recF* or *recR* delayed TLD onset by about 45 min (Fig. 3a). Deletion of *recQ* had a greater effect: killing decreased by ~300 fold after 3 h of T-starvation (Fig. 3b). Thus, ssDNA regions/lesions appear to contribute to TLD.

To obtain direct evidence for accumulation of ssDNA regions during T-starvation, we performed fluorescence microscopy with cells expressing a plasmid-borne gene encoding ssDNA-binding protein (Ssb) fused to yellow fluorescent protein (YFP). Fluorescent foci were detected 30 min after starvation (Fig. 3c). Autofluorescence did not interfere with these measurements, because cells lacking Ssb-YFP expression were completely dark (Supplementary Fig. 2a) and cells expressing Ssb-YFP in the presence of thymidine displayed only a weak, uniform background fluorescence without foci (Fig. 3c–f, time-zero images). As expected[21,34], a double deficiency in *recQ* and *thyA* lowered the prevalence of cells with ssDNA regions during T-starvation. For example, starvation for 30 min increased the prevalence of *ΔthyA* cells having Ssb-YFP fluorescent foci from <1% to >95% (Fig. 3c), while removal of *recQ* from the *ΔthyA* mutant reduced the prevalence of foci (none was seen even after 60 min of starvation; Fig. 3d).

We also examined a deficiency of *rnhA* (RNase HI). This ribonuclease degrades RNA in RNA–DNA hybrids (R-loops) formed during transcription[35], and it can participate in removal of RNA primers associated with lagging-strand DNA synthesis[36,37]. Both processes are expected to increase levels of ssDNA regions[38], and indeed a deficiency in *rnhA* reduced TLD (Fig. 3b). Deletion of *rnhA*, when combined with the *ΔthyA* mutation, also suppressed the formation of ssDNA regions, because the number of fluorescent foci was reduced after T-starvation for 30 min. However, the reduction was not as great as seen with a *recQ* defect: after starvation for 60 min, ~50% of the *ΔthyA-ΔrnhA* double mutant cells exhibited fluorescent foci (Fig. 3e), while for the *ΔthyA-ΔrecQ* mutant the prevalence of foci was <5% (Fig. 3d). Additional work is required to determine whether RNA–DNA hybrids, apart from the generation of ssDNA regions at replication forks, contribute to TLD.

Collectively, the data indicate that mutations expected to protect from TLD by reducing ssDNA regions lower the prevalence of cells exhibiting fluorescent foci originating from regions of ssDNA. Conversely, mutations that protect from TLD by suppressing ROS accumulation (such as *cydB*) had no effect on the prevalence of cells showing ssDNA regions (Fig. 3f and Supplementary Fig. 7a).

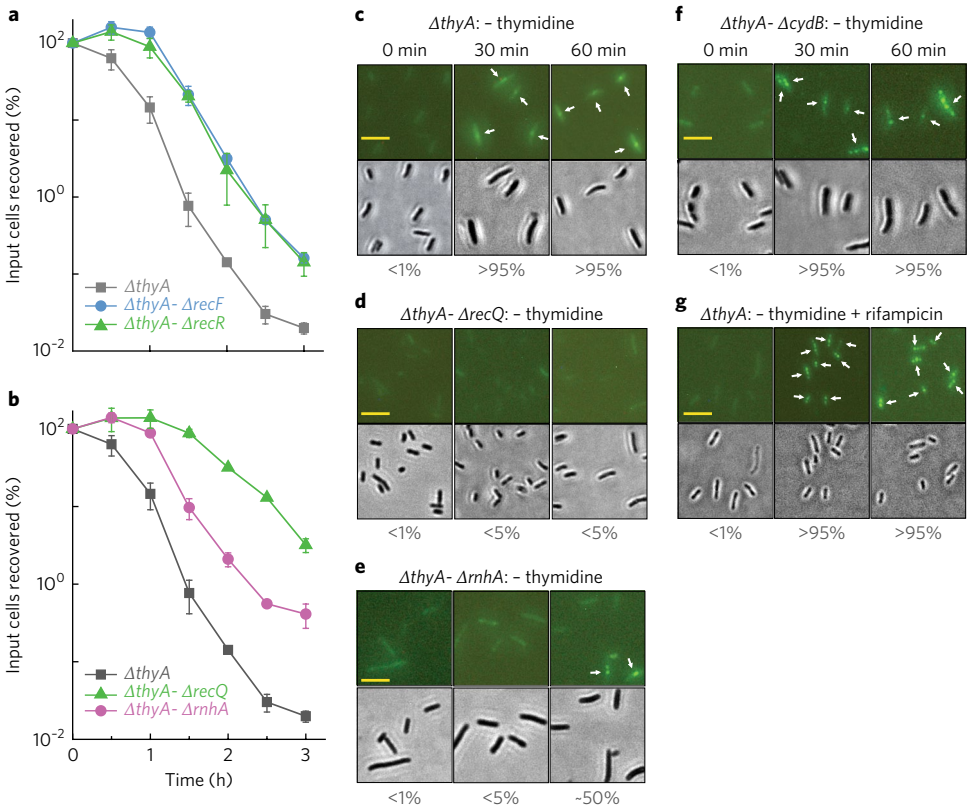

Fig. 3 | ssDNA regions are necessary but insufficient for TLD. a, Effect of deficiencies of RecF or RecR. Mutants deficient in *thyA* and *recF* (strain 3711), *thyA* and *recR* (strain 3955) or only *ΔthyA* (strain 3640) were starved of thymidine, and at the indicated times samples were taken for determination of per cent survival. **b**, Effect of deficiencies in *recQ* and *rnhA*. Mutant strains were starved of thymidine, and at the indicated times per cent survival was determined for *ΔthyA* (strain 3640), *ΔthyA-ΔrecQ* (strain 3952) and *ΔthyA-ΔrnhA* (strain 3664). Data points in **a** and **b** are averages for three independent experiments, and error bars represent standard deviation of the mean. **c**, Prevalence of *ΔthyA* cells (strain 4313) with ssDNA regions. Upper panels: fluorescent foci due to cellular binding of pre-induced Ssb-YFP to ssDNA regions are indicated by arrows. Lower panels: bright-field views of corresponding upper panels. Scale bars (**c**–**g**), 10 μm. Numbers under the panels indicate the prevalence of cells exhibiting fluorescent foci. **d**, Prevalence of *ΔthyA-ΔrecQ* mutant cells with ssDNA regions. Methods were as in **c** but with strain 4335. **e**, Prevalence of *ΔthyA-ΔrnhA* mutant cells exhibiting ssDNA regions. Methods were as in **c** but with strain 4389. **f**, Prevalence of *ΔthyA-ΔcydB* mutant cells exhibiting ssDNA regions. Methods were as in **c** but with strain 4012. **g**, Effect of rifampicin on prevalence of cells with ssDNA. Rifampicin (50 μg ml^{-1}) was added to the *ΔthyA* culture (strain 4313) at the time T-starvation was initiated. Methods were as in **c**. Similar results were observed in three independent experiments for **c**–**g**, and 200 cells for each group were randomly selected for analysis of generation of ssDNA regions.

Because both ROS and ssDNA regions are involved in TLD and because rifampicin reduces ROS accumulation (Fig. 2a) and blocks TLD[13,29,39], we next examined the effect of rifampicin on the accumulation of ssDNA regions during T-starvation. Rifampicin had little effect on the prevalence of cells containing Ssb-YFP fluorescent foci (Fig. 3g and Supplementary Fig. 7a,b). Similarly, treatment with 2,2′-bipyridyl, which suppresses the accumulation of ROS, had little effect on Ssb-YFP foci (Supplementary Figs. 3a and 7c). Thus, ssDNA is required for TLD, but is insufficient (rifampicin blocks TLD but not the formation of ssDNA regions). Because rifampicin also blocks the initiation of replication[15,40] and transcription[41], the data in Fig. 3g indicate that replication and transcription initiation are not required for the accumulation of ssDNA regions during T-starvation.

Conversion of ssDNAs into DNA breaks by ROS underlies TLD. Requiring both ssDNA regions and ROS for TLD fits with the ability of ROS to produce mostly non-lethal, ssDNA cleavage when attacking dsDNA[42]. Only in the rare situation in which two nearby attacks occur, one in each of the two complementary DNA strands, would a double-stranded break arise (Supplementary Fig. 8a). However, ROS attack at ssDNA regions would readily produce DSBs. Thus, an increase in size and/or number of ssDNA regions would increase the production of ROS-mediated DSBs, which may be a major cause of TLD.

Although early work correlated DSB and TLD[9,14,22], a more recent study suggested that rifampicin might inhibit TLD without blocking DNA breakage[13]. Such a conclusion would undermine the idea that DSBs cause TLD. Consequently, we reinvestigated the relationships between DNA breakage and TLD by performing a single-cell assay in which a fusion of *E. coli* RecN and YFP was used to measure the prevalence of cells with DSBs (detection by *E. coli* RecN-YFP was similar to detection by a well-characterized *Bacillus subtilis* RecN-YFP; Supplementary Fig. 9). With the *ΔthyA* mutant growing in thymidine-containing medium or with wild-type cells cultured in thymidine-depleted medium, the prevalence of cells showing RecN-YFP-mediated fluorescent foci was low (<0.1%; Supplementary Fig. 8b). By contrast, T-starvation for 60 min caused almost all *ΔthyA* cells (95%) to exhibit at least one RecN-YFP focus (Fig. 4a). Rifampicin treatment reduced the number of RecN-YPF foci to ~18% (Fig. 4b) while blocking cell death (Supplementary Fig. 8c). Similarly, treatment of starved cells with 2,2′-bipyridyl, which reduces ROS accumulation and TLD (Fig. 1b and Supplementary Fig. 3a), also suppressed DNA breakage (Fig. 4c). Thus, DSBs and an ROS surge correlate with TLD.

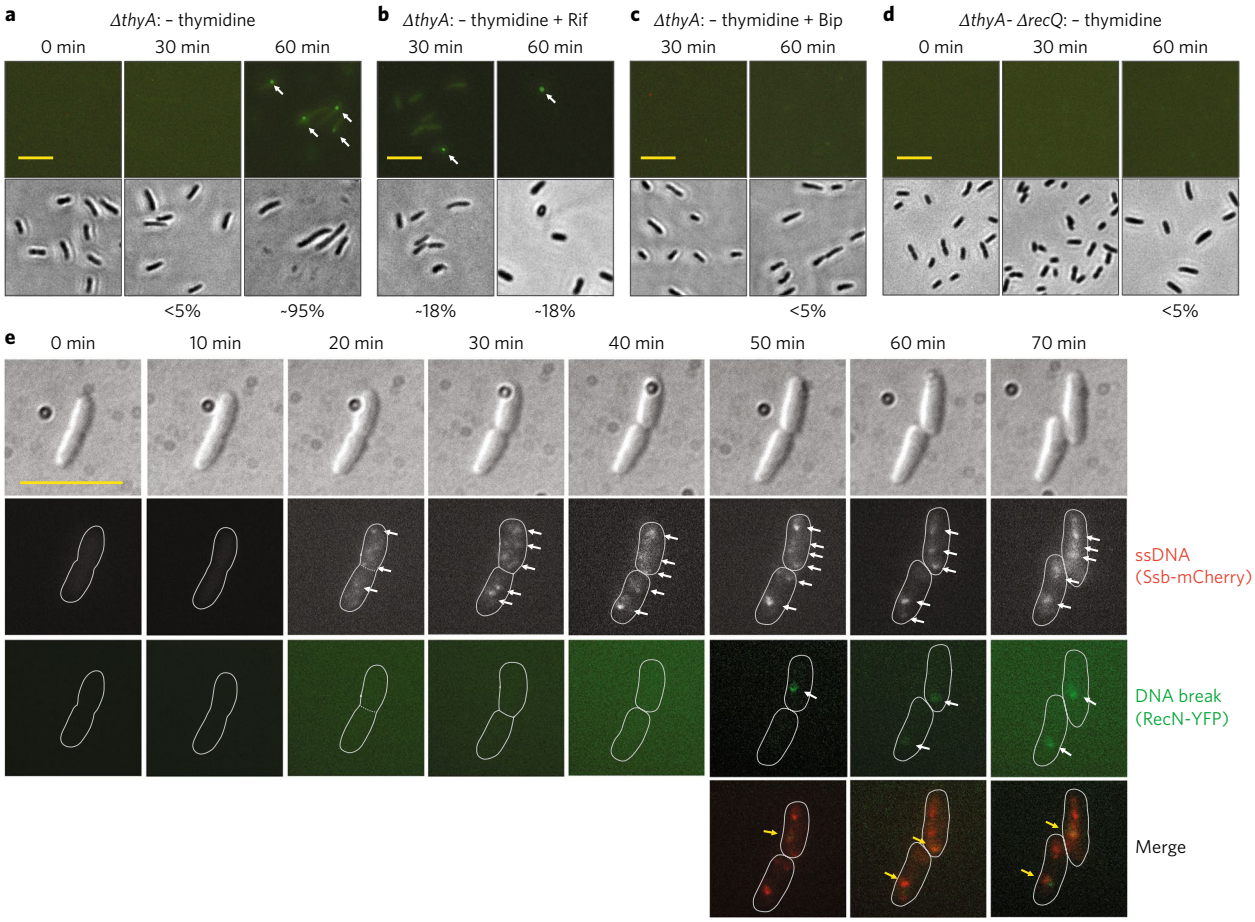

Fig. 4 | dsDNA breaks associated with TLD. a, Prevalence of *ΔthyA* cells with dsDNA breaks during T-starvation. Strain 4258 (*recN-yfp*) was pre-induced with 0.1% arabinose for 2.5 h and then starved of thymidine for the indicated times followed by examination by fluorescence (upper panels) or bright-field microscopy (lower panels). Arrows indicate fluorescent foci. Scale bars (**a**–**e**), 10 μm. Prevalence of cells with at least one fluorescent focus is shown as a percentage below the panels. **b**, Effect of rifampicin on presence of DNA breaks during T-starvation. Methods were as in **a** except that rifampicin (50 μg ml^{-1}) was added immediately after thymidine removal. **c**, Effect of 2,2′-bipyridyl (Bip) on the presence of DNA breaks during T-starvation. Methods were as in **a** except for the addition of 0.5 × MIC Bip immediately after thymidine removal. **d**, Effect of *recQ* on the formation of DNA breaks during T-starvation. Methods were as in **a** but with strain 4262 (*ΔthyA-ΔrecQ*). **e**, Co-localization of DNA breaks and ssDNA regions during T-starvation. Ssb-mCherry was constitutively expressed under the native *ssb* promoter in the chromosome of a *ΔthyA recN-yfp* mutant (strain 4315). Two typical thymidine-starved cells are shown for the appearance of DNA breaks in the ssDNA region. Arrows indicate fluorescent foci. About 60% of DNA breaks (green RecN-YFP foci, $n = 30$) co-localized with regions of ssDNA. All images are typical of pictures obtained from three independent experiments. For **a**–**d**, 200 cells for each group were randomly selected for analysis of the generation of DNA breaks. Detection of dsDNA breaks by *E. coli* RecN was verified by finding the same results with *B. subtilis* RecN expressed in *E. coli* (Supplementary Fig. 9).

Involvement of ssDNA regions in DNA breakage and TLD was also observed when the prevalence of cells with DNA breaks was examined using a *ΔthyA-ΔrecQ* double mutant. A 60 min period of T-starvation with the *ΔthyA* mutant allowed ~95% of the cells to exhibit DSBs (Fig. 4a), but an additional deficiency in *recQ* reduced the number to below 5% (Fig. 4d) and increased survival (Fig. 3b). In summary, reduction in either ROS or ssDNA regions lowers DNA breakage and TLD, but reduction of ROS has little effect on the formation of ssDNA regions (Fig. 3f,g and Supplementary Fig. 7), indicating that ROS do not affect TLD through reduced accumulation of ssDNA regions.

To test the idea that DNA breaks occur in regions of ssDNA, we used fluorescence microscopy to examine co-localization of RecN, which reveals DSBs, and Ssb, which associates with ssDNAs. When we monitored the same thymidine-starved *ΔthyA* cells by microscopy over time, intense Ssb-mCherry foci (ssDNA regions) began to appear 20 min after initiation of T-starvation (Fig. 4e), consistent with our earlier observation of ssDNA accumulation (Fig. 3c). RecN-YFP foci (DSBs) appeared at least 30 min later (Fig. 4a,e), and newly formed breaks co-localized with ssDNA regions (Fig. 4e). Analysis of more than 30 newly formed RecN-YFP foci showed that ~60% of the breaks co-localized with ssDNA regions. Thus, DNA breaks associated with TLD tend to occur at ssDNA regions, as expected from the known action of ROS[42].

We also expected that administering exogenous peroxide would overcome the protection from TLD afforded by reduced production of endogenous ROS. As a test, we first accumulated ssDNA regions by treating thymidine-starved *thyA*-deficient cells with rifampicin for 30 min, which suppressed accumulation of endogenous ROS (Fig. 2a) and eliminated TLD (Supplementary Figs. 8c and 10a), but allowed the formation of ssDNA regions (Fig. 3g). We then treated the cells for an additional 20 min with exogenous H_2O_2 at a concentration that was non-lethal for wild-type cultures or for *ΔthyA* cultures supplemented with thymidine (Supplementary Fig. 10b). Exogenous H_2O_2 reduced the survival of thymidine-starved, rifampicin-treated *ΔthyA* cells from 100% to below 0.1% (Fig. 5a). The exogenous H_2O_2 treatment of thymidine-starved *ΔthyA* cells also raised the fraction of cells with DNA

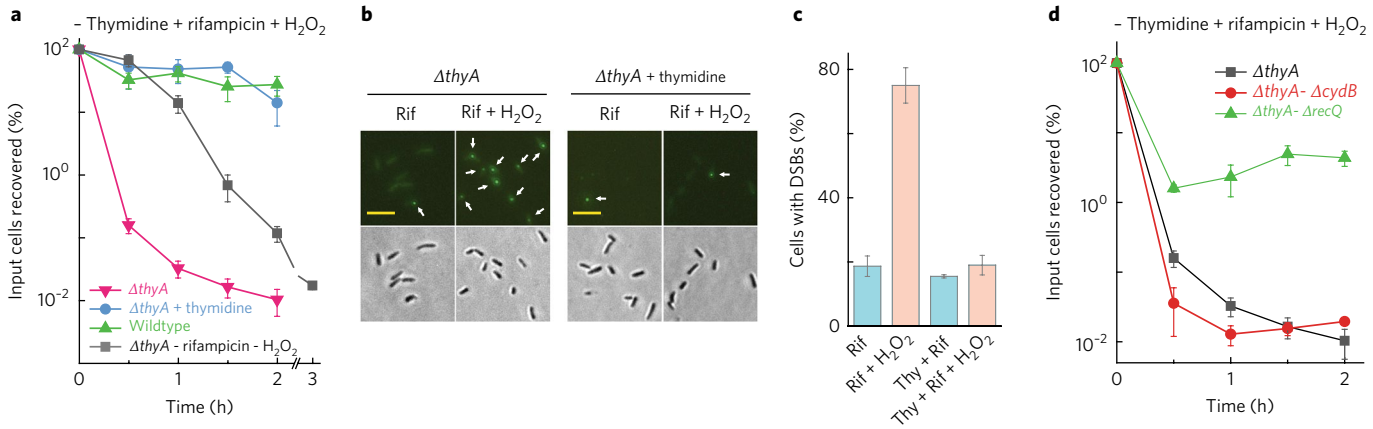

Fig. 5 | Conversion of ssDNA regions into lethal breaks by exogenous ROS. a, Exogenous H_2O_2 reduced survival of rifampicin-treated cells starved of thymidine. Rifampicin was added at the time of thymidine removal. At the indicated times after thymidine removal, H_2O_2 was added to 3.5 mM (unless otherwise indicated) for 20 min before sampling for survival. Squares, *ΔthyA* (strain 3640) without rifampicin or H_2O_2 treatment; circles, *ΔthyA* (strain 3640) incubated with 200 μg ml^{-1} thymidine plus rifampicin and H_2O_2 treatment; triangles, wild-type (strain 3001) plus rifampicin and H_2O_2 treatment; inverted triangles, *ΔthyA* (strain 3640) plus rifampicin and H_2O_2 treatment. **b**, Exogenous H_2O_2 increased the prevalence of cells exhibiting DNA breaks. Plasmid-borne RecN-YFP was pre-induced by 0.1% arabinose for 2.5 h during growth of strain 4282 before removal of thymidine. H_2O_2 (3.5 mM) was added to cultures after 30 min rifampicin treatment and T-starvation. Upper panels: fluorescence after 20 min H_2O_2 treatment. Lower panels: corresponding bright-field views. Scale bars, 10 μm. Microscopy results are representative of three independent experiments. **c**, Prevalence of cells with double-strand breaks generated by exogenous H_2O_2 administered as in **b**. DSB, double-stranded DNA break; Rif, rifampicin; Thy, thymidine. Number of cells examined for the four groups (Rif, Rif + H_2O_2, Thy + Rif and Thy + Rif + H_2O_2) were 1,040, 640, 460 and 1,190 cells, respectively. Data from three independent experiments were used for analysis. **d**, Effect of *recQ* and *cydB* deficiencies on survival of rifampicin-treated, thymidine-starved *ΔthyA* cells when exposed to exogenous H_2O_2. H_2O_2 treatment was as in **a**. Squares, *ΔthyA* (strain 3640); circles, *ΔthyA-ΔcydB* (strain 4012); triangles, *ΔthyA-ΔrecQ* (strain 3952). Error bars in **a**, **c** and **d** represent standard deviation of the mean determined from three independent experiments.

breaks (RecN-YFP foci) from ~18% to 75% (Fig. 5b,c). When thymidine was present, H_2O_2 did not trigger a surge in DNA breaks in the *ΔthyA* mutant (Fig. 5b,c). Collectively these data support the conclusion that conversion of ssDNA regions into DSBs by endogenous ROS is a major cause of TLD.

If TLD derives from ROS-mediated conversion of ssDNA regions into DSBs, exogenous H_2O_2-mediated killing should be mitigated by perturbations that reduce the number and/or size of ssDNA regions. Indeed, deficiencies in *recQ* and *rnhA* protected *E. coli* from exogenous peroxide-mediated killing of rifampicin-treated, thymidine-starved cultures (Fig. 5d and Supplementary Fig. 10c). By contrast, mutants deficient in genes such as *cydB* and *ubiG*, which reduce intracellular ROS but not ssDNA regions, allowed killing by exogenous peroxide (Figs. 2c, 3f, 5d and Supplementary Fig. 10d). These observations fit with ROS converting elevated levels of persistent ssDNA regions, arising from T-starvation, into DSBs associated with rapid cell death.

The temporal order of the appearance of ssDNA regions, ROS, DSBs, and cell death also supports TLD arising from ROS-mediated breakage of DNA in ssDNA regions; accumulation of ssDNA regions was seen at 30 min of T-starvation, whereas the ROS surge, DSBs, and death were not obvious until 60 min after starvation (Supplementary Fig. 11). DNA breaks and the ROS surge appeared at the same time, and both continued to accumulate as survival decreased. By contrast, ssDNA regions tended to saturate after 30 min of starvation (Supplementary Fig. 11).

Discussion

The work described above adds ROS to explanations of TLD. Two pathways (Fig. 6) converge to generate lethal dsDNA breaks. In one, T-starvation leads to persistent ssDNA regions/lesions that are expanded by RecF and RecQ. In the other, an undefined signal stimulates ROS accumulation; elevated levels of ROS then convert ssDNA into DNA breaks. Attempts to repair breaks involve genes, such as *recBC* and *ruvABC*, that, when deficient, render cells hypersensitive to T-starvation[6,9,11,14]. Moreover, RecA/RecFOR-mediated toxic recombination may occur[6,9,10], which can be mitigated by UvrD antagonizing RecAFOR function[9,11]. As pointed out above, RecQ/RecFOR may facilitate TLD by promoting/expanding ssDNA regions that serve as substrates for ROS-mediated lethal DSB production. Induction of the SOS response would then activate the SulA checkpoint that blocks cell growth on thymine-containing agar during survival measurement[6]. A double deficiency of *mutM* and *mutY*, genes that are responsible for removal of 8-oxo-dGTP[43], showed a two- to fourfold protection from TLD, while overexpression of *mutT* (encoding an 8-oxo-dGTP sanitizer) exhibited little protection (Supplementary Fig. 12), unlike the large protective effect observed with antimicrobial killing[43]. Several other repair genes, such as *ung*, *uvrA* and *mutS*[9,11], showed no effect. Collectively, these data suggest that excision of incorrect or damaged bases has, at most, a minor contribution to TLD.

Several lines of work support the two pathways in Fig. 6. First, accumulation of ROS is lowered and TLD is blocked/reduced by treatment with rifampicin, chloramphenicol, an iron chelator, a radical scavenger, and deletion of respiratory genes. Second, deficiencies in enzymes that normally reduce levels of peroxide increase the rate and extent of TLD. Third, regions of ssDNA persist when replication is halted by T-starvation[22] and are probably expanded by RecF and RecQ[7,21,33]; RNaseH, which generates single-stranded regions of DNA[38], also contributes to TLD. Other potential sources of ssDNA involve attempts to repair nicks created by a variety of sources (for example, ROS[44], transcription[45], base misincorporation[18], and base oxidation[43]). Fourth, DNA breaks co-localize with regions of ssDNA, and sublethal exogenous H_2O_2 becomes lethal under conditions that allow T-starvation to accumulate ssDNA lesions but an insufficient level of endogenous ROS. Finally, TLD was largely abolished when ROS were reduced to background levels by a respiratory deficiency plus either an iron chelator or *ΔrecF* (Fig. 2d and Supplementary Fig. 6). Thus, most, if not all, of TLD depends on ROS under nutrient-rich conditions.

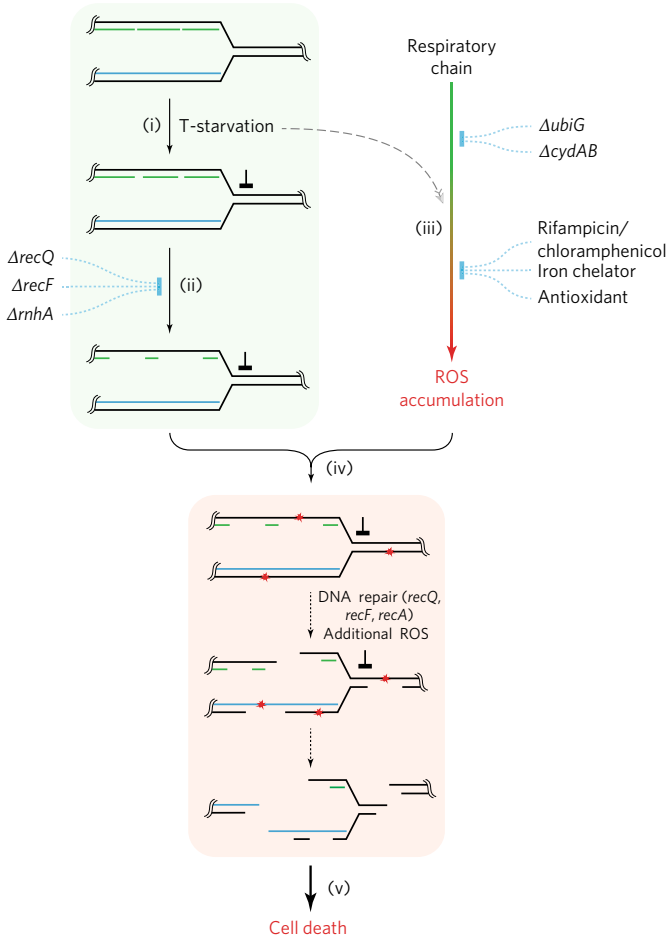

Fig. 6 | Scheme describing ROS-mediated conversion of ssDNA regions into lethal DSBs during TLD. (i) When growing cells are starved of thymine, DNA replication forks stall. They then advance slowly by recruiting thymine from degraded DNA. (ii) ssDNA regions, located in the lagging strands behind replication forks and at sites of single-strand lesion repair, enlarge due to attempted repair in the absence of dTTP. The number and size of ssDNA regions increase due to DNA-damage-repair systems (RecQ/RecFOR) and due to degradation of RNA from RNA–DNA hybrids (RnhA). (iii) T-starvation triggers accumulation of intracellular ROS as byproducts of respiration. Disruption of the respiratory chain by deletion of *ubiG* or *cydAB* decreases ROS generation. Addition of RNA or protein synthesis-inhibiting agents (rifampicin or chloramphenicol) inhibits cell respiration, thereby suppressing the ROS surge. ROS accumulation is also inhibited by the presence of Fe^{2+} chelators such as 2,2′-bipyridyl, or antioxidants such as DMSO. These ROS-inhibiting agents have little effect on expansion of ssDNA regions. (iv) DNA is attacked by ROS, especially hydroxyl radical. When ROS attack occurs in ssDNA regions, DSBs arise. ROS-mediated attack of dsDNA leads primarily to single-strand lesions, which could be expanded into large single-strand regions by abortive DNA repair in the absence of dTTP. (v) Extensive DNA breakage results in cell death, with deficiencies in DSB repair exacerbating TLD[11]. Induction of SOS/*sulA*, which may occur at multiple steps in the scheme, can lower the ability of cells to resume growth after thymine becomes available[6].

The inhibitory effects of rifampicin on TLD are complex. Because this drug inhibits transcription and TLD, an argument can be made that, during T-starvation, transcription converts ssDNA regions to DSBs. However, transcription cannot be sufficient for TLD, because it is expected to occur even when TLD is largely blocked by bipyridyl treatment of a *ΔthyA-ΔubiG* mutant or by combination of *ΔthyA* with *ΔcydB* and *ΔrecF* during T-starvation. Another issue is that our in vivo single-cell-based microscopy study showed that rifampicin inhibits DNA breakage, which contradicts previous work using a batch culture-based gel electrophoresis assay[13]. The latter assay suffers from technical ambiguities. For example, T-starvation may generate complex DNA structures[7,46] that might not form during rifampicin treatment[47], thereby allowing rifampicin-treated samples to enter the gel more readily than rifampicin-untreated ones. Another feature of rifampicin is its inability to block the accumulation of ssDNA regions during T-starvation. Even though rifampicin blocks the initiation of replication and transcription[15,40,41], it does not block death from concentrations of exogenous peroxide that are normally non-lethal. Thus, initiation of replication or transcription is not required for accumulation of ssDNA regions or TLD when cells are grown in nutrient-rich medium.

We consider TLD to be an example of bacterial self-destruction that occurs when stress is severe. The process is an active one, because transcription, translation and DNA-damage repair systems are involved[1,6,9,11,14,18]. Other examples of self-destruction include part of the lethal activity associated with diverse antimicrobials[23,25,26]. With antimicrobial-mediated killing, a pathway to ROS accumulation is thought to include toxin–antitoxin (TA) modules (such as MazEF), the two-component CpxAR and ArcAB systems, a small regulatory RNA (tmRNA, encoded by *ssrA*) and the ClpAP protease[25,26,48,49]. However, ROS and TLD are unaffected by the absence of TA modules (Supplementary Fig. 13a–d); moreover, disruption of *arcA/B*, *lon*, *clpA/P*, *cpxA/R* or *ssrA* has little effect on TLD (Supplementary Fig. 13e–i). Thus, the pathways to TLD and antimicrobial-mediated death differ in how they elicit ROS accumulation. Nevertheless, surges in ROS and involvement of the respiratory chain are shared features[23,31,50], as is the presence of metabolically inert, persister subpopulations that tolerate many types of lethal stress. The next challenge is to learn how bacterial cells sense the macromolecular lesions that stimulate a self-destructive ROS surge.

Methods

Bacterial strains, growth conditions and reagents. *E. coli* strains (Supplementary Table 1) were grown aerobically in Hi-DEF Azure medium (Teknova) or in M9 minimal medium with 1% glucose, both with 50 μg ml^{-1} thymidine at 37 °C unless specified otherwise. Thermo Fisher Scientific supplied ROS-sensitive dyes: 5(6)-carboxy-2′,7′-dichlorodihydrofluorescein diacetate (carboxy-H2DCFDA, which penetrates cells in its parental form but cannot exit the cell once the compound is cleaved by cellular esterases[51]), 2′,3′,6′,7′-tetrahydro-12′-(4,4,5,5-tetramethyl-1,3,2-dioxaborolan-2-yl)-spiro[isobenzofuran-1(3*H*),9′-[1*H*,5*H*,9*H*]xantheno[2,3,4-ij]quinolizin]-3-one (Peroxy Orange-1) and 4,4-difluoro-5-(4-phenyl-1,3-butadienyl)-4-bora-3a,4a-diaza-*s*-indacene-3-undecanoic acid (C11-BODIPY). Other reagents were obtained from Sigma-Aldrich.

Thymidine starvation and bacterial survival measurement. Overnight cultures were diluted 200-fold into fresh medium, grown to log phase (A_{600} (absorbance at 600 nm) = 0.15) with rotary shaking at 250 r.p.m., collected by centrifugation (8,000 *g* for 30 s), and washed with the same volume of saline (0.9% NaCl) at room temperature to remove thymidine. Cell pellets from 1 ml cultures were suspended in 2 ml fresh medium lacking thymidine. When appropriate, 2,2′-bipyridyl or DMSO was added to a final, sub-inhibitory concentration of 0.35 mM or 700 mM (0.5 × MIC (minimum inhibitory concentration)), respectively. Cultures were immediately shifted to 37 °C with shaking to initiate T-starvation. All survival data were normalized to cell density (2 to 5 × 10^7 c.f.u. ml^{-1}) at the time starvation was initiated to facilitate comparisons of experiments.

For TLD during anaerobiosis, the *thyA* mutant was grown in Hi-DEF Azure medium containing 50 mM fumarate and 50 μg ml^{-1} thymidine in a sealed Vacutainer blood-draw tube (BD Medical Supplies) through which Bioblend anaerobic gas (10% H_2, 5% CO_2, 85% N_2; Welco Gas Corp) was passed for 30 min via a long inlet needle submerged in the medium and a short outlet needle at the top of the head space of the tube. Both needles passed through the rubber stopper of the Vacutainer tube, which was sealed when the needles were removed. When the culture density reached an A_{600} of 0.15, cells were concentrated by centrifugation, resuspended in medium lacking thymidine, and pretreated with Bioblend anaerobic gas in a Vacutainer tube for 30 min. Aliquots were removed via syringe through the inlet needle, diluted in saline containing 50 μg ml^{-1} thymidine, applied to LB (Luria-Bertani) agar containing thymidine, and incubated overnight in ambient air to determine colony-forming units (c.f.u.).

H_2O_2 was used to overcome the inhibitory effect of rifampicin on TLD by growing bacteria to $A_{600}=0.15$ in Hi-DEF Azure medium with 50 μg ml^{-1} thymidine, adding rifampin to 5×MIC (50 μg ml^{-1}) when cells were suspended in fresh medium lacking thymidine, and at various times adding H_2O_2 to 3.5 mM. After H_2O_2 treatment for 20 min, aliquots were removed for c.f.u. determination.

Flow cytometry. Bacterial fluorescence intensity was determined using fluorescence-based flow cytometry. Carboxy-H2DCFDA (10 μM), Peroxy Orange-1 (5 μM), or C11-BODIPY (2 μM) was present in the growth medium to detect overall intracellular ROS, H_2O_2, or lipid peroxidation, respectively[51–53]. A no-dye sample was included to control for autofluorescence. A total of 100,000 ungated events for each time-point sample was determined by a BD Accuri C6 Plus flow cytometer (Becton Dickinson) using the following detection parameters: 20 mV laser power, 533/30 nm band-pass filter (FL1-channel) for carboxy-H2DCFDA and 585/40 nm band-pass filter (FL2-channel) for Peroxy Orange-1 and C11-BODIPY. Data were analysed using BD Accuri C6 software.

Visualization of DNA lesions. *E. coli* cells containing ss- or dsDNA breaks were detected by fluorescence microscopy using YFP fused to ssDNA-binding protein (Ssb) or RecN. The ability of *E. coli* RecN to detect dsDNA breaks was validated by comparison with *B. subtilis* RecN-YFP expressed in the *E. coli thyA* mutant (*E. coli* RecN displayed the same extent of DSB foci as the well-characterized RecN from *B. subtilis* when expressed in *E. coli* as RecN-YFP fusions[54]; Supplementary Fig. 9). *recN-yfp* was introduced into *E. coli* strains by transduction to replace native *recN*. Log-phase cultures of *E. coli* were starved for thymidine, as above (see section 'Thymidine starvation and bacterial survival measurement'), to initiate TLD. Samples taken at various times were concentrated ten-fold by centrifugation (9,000 *g* for 20 s), mixed with 1/3 volume 1.5% low-melting-point agarose (FMC) at 40 °C, and immediately spread on a microscope slide.

For visualization of cells containing DNA breaks caused by exogenous H_2O_2, *recN-yfp* was cloned into plasmid pBAD18 between the *Eco* RI and *Hind* III sites to generate pBAD18-*recN-yfp*. For visualization of cells with ssDNA regions, the open reading frames of *ssb* (lacking a stop codon) and *yfp* were cloned into pBAD18 between the *Eco* RI and *Kpn* I sites and between the *Sal* I and *Hind* III sites, respectively, to generate pBAD18-*ssb-yfp*. Plasmid-expressed Ssb-YFP revealed ssDNA regions as fluorescent foci[55] (wild-type *ssb* was maintained in the chromosome). Recombinant plasmids were introduced separately into wild-type and *ΔthyA* strains by bacterial transformation using electroporation. Thymine starvation, rifampicin treatment, and H_2O_2 treatment were as described above (see section 'Thymidine starvation and bacterial survival measurement'). Samples were removed after 20 min of peroxide treatment, washed with saline, and concentrated ten-fold by centrifugation.

Microscopy was performed with a Nikon Eclipse TS100 inverted microscope with filters for excitation and emission of YFP, and carboxy-H2DCFDA. Automated unbiased image acquisition was carried out with NIS Elements BR imaging software (Nikon).

Co-localization of DNA breaks with ssDNA regions. For visualization of DNA breaks occurring in ssDNA regions within the same cell, *recN-yfp* and *ssb-mCherry* were introduced into the genome of the *ΔthyA* mutant to replace their native genes using bacteriophage P1-mediated transduction. After removal of thymidine, cells of strain 4496, grown to mid-log phase, were concentrated ten-fold by centrifugation (9,000 *g* for 20 s), and spotted onto an agarose pad on a microscope slide (prepared with fresh medium lacking thymidine, as described previously[56]). Slides with cells were immediately placed on a Zeiss Axiovert 200M microscope, where they were kept at ~35 °C. DNA breaks (RecN-YFP), and ssDNA regions (Ssb-mCherry) in cells within the same field of view were recorded every 10 min.

Statistical considerations. All experiments were performed with at least three independent biological replicates. Three technical replicates were included for each sample point. Each value was presented as the mean value of the biological replicates, with standard deviation shown as error bars. At least five time points were chosen for each kinetic experiment to cover a wide range. *P* values were not presented, because our data sought kinetic trends with greater than ten-fold differences in cell survival at multiple time points and qualitative differences in microscopic images and flow cytometry profiles.

Data availability. Data supporting the findings of this study are shown in the main text and in the Supplementary Information and are available from the corresponding author upon request. No sequence, structure or omics data required to be deposited in a public repository were generated in the study. Bacterial mutant strains and plasmids constructed in this work are listed in Supplementary Table 1 and are available upon request.

Received: 7 November 2016; Accepted: 5 September 2017;
Published online: 02 October 2017

References

1. Ahmad, S. I., Kirk, S. H. & Eisenstark, A. Thymine metabolism and thymineless death in prokaryotes and eukaryotes. *Annu. Rev. Microbiol.* **52**, 591–625 (1998).
2. Cohen, S. S. & Barner, H. D. Studies on unbalanced growth in *Escherichia coli*. *Proc. Natl Acad. Sci. USA* **40**, 885–893 (1954).
3. Smith, D. W. & Hanawalt, P. C. Macromolecular synthesis and thymineless death in *Mycoplasma laidlawii* B. *J. Bacteriol.* **96**, 2066–2076 (1968).
4. Sat, B., Reches, M. & Engelberg-Kulka, H. The *Escherichia coli mazEF* suicide module mediates thymineless death. *J. Bacteriol.* **185**, 1803–1807 (2003).
5. Kunz, B. A. & Glickman, B. W. Mechanism of mutation by thymine starvation in *Escherichia coli*: clues from mutagenic specificity. *J. Bacteriol.* **162**, 859–864 (1985).
6. Fonville, N. C., Bates, D., Hastings, P. J., Hanawalt, P. C. & Rosenberg, S. M. Role of RecA and the SOS response in thymineless death in *Escherichia coli*. *PLoS Genet.* **6**, e1000865 (2010).
7. Nakayama, K., Kusano, K., Irino, N. & Nakayama, H. Thymine starvation-induced structural changes in *Escherichia coli* DNA. Detection by pulsed field gel electrophoresis and evidence for involvement of homologous recombination. *J. Mol. Biol.* **243**, 611–620 (1994).
8. Pauling, C. & Hanawalt, P. Nonconservative DNA replication in bacteria after thymine starvation. *Proc. Natl Acad. Sci. USA* **54**, 1728–1735 (1965).
9. Kuong, K. J. & Kuzminov, A. Stalled replication fork repair and misrepair during thymineless death in *Escherichia coli*. *Genes Cells* **15**, 619–634 (2010).
10. Magner, D. B. et al. RecQ promotes toxic recombination in cells lacking recombination intermediate-removal proteins. *Mol. Cell* **26**, 273–286 (2007).
11. Fonville, N. C., Vaksman, Z., DeNapoli, J., Hastings, P. J. & Rosenberg, S. M. Pathways of resistance to thymineless death in *Escherichia coli* and the function of UvrD. *Genetics* **189**, 23–36 (2011).
12. Sangurdekar, D. P. et al. Thymineless death is associated with loss of essential genetic information from the replication origin. *Mol. Microbiol.* **75**, 1455–1467 (2010).
13. Martin, C. M. & Guzman, E. C. DNA replication initiation as a key element in thymineless death. *DNA Repair* **10**, 94–101 (2011).
14. Kuong, K. J. & Kuzminov, A. Disintegration of nascent replication bubbles during thymine starvation triggers RecA- and RecBCD-dependent replication origin destruction. *J. Biol. Chem.* **287**, 23958–23970 (2012).
15. Martin, C. M., Viguera, E. & Guzman, E. C. Rifampicin suppresses thymineless death by blocking the transcription-dependent step of chromosome initiation. *DNA Repair* **18**, 10–17 (2014).
16. Morganroth, P. A. & Hanawalt, P. C. Role of DNA replication and repair in thymineless death in *Escherichia coli*. *J. Bacteriol.* **188**, 5286–5288 (2006).
17. Hamilton, H. M. et al. Thymineless death is inhibited by CsrA in *Escherichia coli* lacking the SOS response. *DNA Repair* **12**, 993–999 (2013).
18. Khodursky, A., Guzman, E. C. & Hanawalt, P. C. Thymineless death lives on: new insights into a classic phenomenon. *Annu. Rev. Microbiol.* **69**, 247–263 (2015).
19. Nakayama, H. et al. Isolation and genetic characterization of a thymineless death-resistant mutant of *Escherichia coli* K12: identification of a new mutation (*recQ1*) that blocks the RecF recombination pathway. *Mol. Gen. Genet.* **195**, 474–480 (1984).
20. Nakayama, K., Shiota, S. & Nakayama, H. Thymineless death in *Escherichia coli* mutants deficient in the RecF recombination pathway. *Can. J. Microbiol.* **34**, 905–907 (1988).
21. Courcelle, J. & Hanawalt, P. C. RecQ and RecJ process blocked replication forks prior to the resumption of replication in UV-irradiated *Escherichia coli*. *Mol. Gen. Genet.* **262**, 543–551 (1999).
22. Ayusawa, D., Shimizu, K., Koyama, H., Takeishi, K. & Seno, T. Accumulation of DNA strand breaks during thymineless death in thymidylate synthase-negative mutants of mouse FM3A cells. *J. Biol. Chem.* **258**, 12448–12454 (1983).
23. Kohanski, M. A., Dwyer, D. J., Hayete, B., Lawrence, C. A. & Collins, J. J. A common mechanism of cellular death induced by bactericidal antibiotics. *Cell* **130**, 797–810 (2007).
24. Dorsey-Oresto, A. et al. YihE kinase is a central regulator of programmed cell death in bacteria. *Cell Rep.* **3**, 528–537 (2013).
25. Zhao, X. & Drlica, K. Reactive oxygen species and the bacterial response to lethal stress. *Curr. Opin. Microbiol.* **21**, 1–6 (2014).
26. Dwyer, D. J., Collins, J. J. & Walker, G. C. Unraveling the physiological complexities of antibiotic lethality. *Annu. Rev. Pharmacol. Toxicol.* **55**, 313–332 (2015).
27. Demougeot, C. et al. Cytoprotective efficacy and mechanisms of the liposoluble iron chelator 2,2′-dipyridyl in the rat photothrombotic ischemic stroke model. *J. Pharmacol. Exp. Ther.* **311**, 1080–1087 (2004).
28. Beckman, J. S., Beckman, T. W., Chen, J., Marshall, P. A. & Freeman, B. A. Apparent hydroxyl radical production by peroxynitrite: implications for endothelial injury from nitric oxide and superoxide. *Proc. Natl Acad. Sci. USA* **87**, 1620–1624 (1990).
29. Hanawalt, P. C. Involvement of synthesis of RNA in thymineless death. *Nature* **198**, 286 (1963).

30. Pinney, R. J. & Smith, J. T. R factor elimination during thymine starvation: effects of inhibition of protein synthesis and readdition of thymine. *J. Bacteriol.* **111**, 361–367 (1972).
31. Lobritz, M. A. et al. Antibiotic efficacy is linked to bacterial cellular respiration. *Proc. Natl Acad. Sci. USA* **112**, 8173–8180 (2015).
32. Borisov, V. B. et al. Aerobic respiratory chain of *Escherichia coli* is not allowed to work in fully uncoupled mode. *Proc. Natl Acad. Sci. USA* **108**, 17320–17324 (2011).
33. Morimatsu, K. & Kowalczykowski, S. C. RecFOR proteins load RecA protein onto gapped DNA to accelerate DNA strand exchange: a universal step of recombinational repair. *Mol. Cell* **11**, 1337–1347 (2003).
34. Morimatsu, K. & Kowalczykowski, S. C. RecQ helicase and RecJ nuclease provide complementary functions to resect DNA for homologous recombination. *Proc. Natl Acad. Sci. USA* **111**, E5133–E5142 (2014).
35. Crooke, S. T. et al. Kinetic characteristics of *Escherichia coli* RNase H1: cleavage of various antisense oligonucleotide–RNA duplexes. *Biochem. J.* **312**(Pt 2), 599–608 (1995).
36. Kitani, T., Yoda, K. Y., Ogawa, T. & Okazaki, T. Evidence that discontinuous DNA-replication in *Escherichia coli* is primed by approximately 10 to 12 residues of RNA starting with a purine. *J. Mol. Biol.* **184**, 45–52 (1985).
37. Ogawa, T. & Okazaki, T. Function of RNase H in DNA replication revealed by RNase H defective mutants of *Escherichia coli*. *Mol. Gen. Genet.* **193**, 231–237 (1984).
38. Shimamoto, T., Shimada, M., Inouye, M. & Inouye, S. The role of ribonuclease H in multicopy single-stranded DNA synthesis in retron-Ec73 and retron-Ec107 of *Escherichia coli*. *J. Bacteriol.* **177**, 264–267 (1995).
39. Nakayama, H. & Hanawalt, P. Sedimentation analysis of deoxyribonucleic acid from thymine-starved *Escherichia coli*. *J. Bacteriol.* **121**, 537–547 (1975).
40. Lark, K. G. Evidence for the direct involvement of RNA in the initiation of DNA replication in *Escherichia coli* 15T. *J. Mol. Biol.* **64**, 47–60 (1972).
41. Campbell, E. A. et al. Structural mechanism for rifampicin inhibition of bacterial RNA polymerase. *Cell* **104**, 901–912 (2001).
42. Kobayashi, S., Ueda, K. & Komano, T. The effects of metal ions on the DNA damage induced by hydrogen peroxide. *Agric. Biol. Chem.* **54**, 69–76 (1990).
43. Foti, J. J., Devadoss, B., Winkler, J. A., Collins, J. J. & Walker, G. C. Oxidation of the guanine nucleotide pool underlies cell death by bactericidal antibiotics. *Science* **336**, 315–319 (2012).
44. Cadet, J., Ravanat, J. L., TavernaPorro, M., Menoni, H. & Angelov, D. Oxidatively generated complex DNA damage: tandem and clustered lesions. *Cancer Lett.* **327**, 5–15 (2012).
45. Hanawalt, P. C. et al. Repair replication of DNA *in vivo*. *Cold Spring Harb. Symp. Quant. Biol.* **33**, 187–194 (1968).
46. Bendich, A. J. The form of chromosomal DNA molecules in bacterial cells. *Biochimie* **83**, 177–186 (2001).
47. Hecht, R. M. & Pettijohn, D. E. Studies of DNA bound RNA molecules isolated from nucleoids of *Escherichia coli*. *Nucleic Acids Res.* **3**, 767–788 (1976).
48. Kohanski, M. A., Dwyer, D. J., Wierzbowski, J., Cottarel, G. & Collins, J. J. Mistranslation of membrane proteins and two-component system activation trigger antibiotic-mediated cell death. *Cell* **135**, 679–690 (2008).
49. Li, L. et al. Ribosomal elongation factor 4 promotes cell death associated with lethal stress. *mBio* **5**, e01708 (2014).
50. Davies, B. W. et al. Hydroxyurea induces hydroxyl radical-mediated cell death in *Escherichia coli*. *Mol. Cell* **36**, 845–860 (2009).
51. Bass, D. A. et al. Flow cytometric studies of oxidative product formation by neutrophils: a graded response to membrane stimulation. *J. Immunol.* **130**, 1910–1917 (1983).
52. Dickinson, B. C. & Chang, C. J. Chemistry and biology of reactive oxygen species in signaling or stress responses. *Nat. Chem. Biol.* **7**, 504–511 (2011).
53. Drummen, G. P., van Liebergen, L. C., Op den Kamp, J. A. & Post, J. A. C11-BODIPY$^{581/591}$, an oxidation-sensitive fluorescent lipid peroxidation probe: (micro)spectroscopic characterization and validation of methodology. *Free Radic. Biol. Med.* **33**, 473–490 (2002).
54. Kidane, D., Sanchez, H., Alonso, J. C. & Graumann, P. L. Visualization of DNA double-strand break repair in live bacteria reveals dynamic recruitment of *Bacillus subtilis* RecF, RecO and RecN proteins to distinct sites on the nucleoids. *Mol. Microbiol.* **52**, 1627–1639 (2004).
55. Youngren, B., Nielsen, H. J., Jun, S. & Austin, S. The multifork *Escherichia coli* chromosome is a self-duplicating and self-segregating thermodynamic ring polymer. *Genes Dev.* **28**, 71–84 (2014).
56. Skinner, S. O., Sepulveda, L. A., Xu, H. & Golding, I. Measuring mRNA copy number in individual *Escherichia coli* cells using single-molecule fluorescent in situ hybridization. *Nat. Protoc.* **8**, 1100–1113 (2013).

Acknowledgements

The authors thank G.C. Walker, S.M. Rosenberg, K. Gerdes, D. Jin, J. Imlay and H. Aiba for strains and D. Dubnau, J. Freundlich, M. Gennaro, M. Neiditch and B. Shopsin for critical comments on the manuscript. The authors also acknowledge support from grants from the National Institutes of Health (DP2OD007423 and R01 AI07341) and the National Natural Science Foundation of China (81473251).

Author contributions

Y.H. conducted most of the experiments. Y.H., L.L. and G.L. conducted flow cytometry and microscopy assays. Y.H., L.L., G.L., K.D. and X.Z. analysed the data. Y.H., K.D. and X.Z. designed the study and wrote the manuscript.

Competing interests

The authors declare no competing financial interests.

Additional information

Supplementary information is available for this paper at https://doi.org/10.1038/s41564-017-0037-y.

Reprints and permissions information is available at www.nature.com/reprints.

Correspondence and requests for materials should be addressed to X.Z.

Publisher's note: Springer Nature remains neutral with regard to jurisdictional claims in published maps and institutional affiliations.

nature research

Corresponding author(s): Xilin Zhao

☐ Initial submission ☐ Revised version ☒ Final submission

Life Sciences Reporting Summary

Nature Research wishes to improve the reproducibility of the work that we publish. This form is intended for publication with all accepted life science papers and provides structure for consistency and transparency in reporting. Every life science submission will use this form; some list items might not apply to an individual manuscript, but all fields must be completed for clarity.

For further information on the points included in this form, see Reporting Life Sciences Research. For further information on Nature Research policies, including our data availability policy, see Authors & Referees and the Editorial Policy Checklist.

Experimental design

1. Sample size

   Describe how sample size was determined.

   All experiments were performed with at least three independent biological replicates. Three technical replicates were included for each sample point. Each value shown in figures was presented as the mean value of the biological replicates, with standard deviation shown as error bars. At least 5 time points were chosen for each kinetic experiment to cover a wide range. p-values were not presented, since our data sought kinetic trends having greater than 10-fold differences in cell survival at multiple time points and qualitative differences in microscopic images and flow cytometry profiles.

2. Data exclusions

   Describe any data exclusions.

   No exclusion.

3. Replication

   Describe whether the experimental findings were reliably reproduced.

   All attempts at replication were successful.

4. Randomization

   Describe how samples/organisms/participants were allocated into experimental groups.

   For microscopy assays, more than 200 cells from each experimental group were randomly selected for determination of the percentage of cells having DNA breaks.

5. Blinding

   Describe whether the investigators were blinded to group allocation during data collection and/or analysis.

   No blinding was carried out, since our experiments do not involve animals or human subjects. Moreover, the E. coli cultures used in our work have different genotypes and they need to be grown/treated with different conditions, which makes blinding difficult and unnecessary.

Note: all studies involving animals and/or human research participants must disclose whether blinding and randomization were used.

6. Statistical parameters

For all figures and tables that use statistical methods, confirm that the following items are present in relevant figure legends (or in the Methods section if additional space is needed).

n/a	Confirmed
☐	☒ The exact sample size (*n*) for each experimental group/condition, given as a discrete number and unit of measurement (animals, litters, cultures, etc.)
☐	☒ A description of how samples were collected, noting whether measurements were taken from distinct samples or whether the same sample was measured repeatedly
☐	☒ A statement indicating how many times each experiment was replicated
☒	☐ The statistical test(s) used and whether they are one- or two-sided (note: only common tests should be described solely by name; more complex techniques should be described in the Methods section)
☒	☐ A description of any assumptions or corrections, such as an adjustment for multiple comparisons
☒	☐ The test results (e.g. *P* values) given as exact values whenever possible and with confidence intervals noted
☐	☒ A clear description of statistics including central tendency (e.g. median, mean) and variation (e.g. standard deviation, interquartile range)
☐	☒ Clearly defined error bars

See the web collection on statistics for biologists for further resources and guidance.

Software

Policy information about availability of computer code

7. Software

Describe the software used to analyze the data in this study.

Flow cytometry data were analyzed by the BD Accuri C6 software and then were exported to FlowJo for figure preparation. Images from microscopy were captured by the NIS Elements BR imaging software or OpenLab. Images were then cropped using Photoshop for showing representative bacterial cells. Standard deviations and standard errors were analyzed by Origin. All panels were arranged into figures in Adobe Illustrator.

For manuscripts utilizing custom algorithms or software that are central to the paper but not yet described in the published literature, software must be made available to editors and reviewers upon request. We strongly encourage code deposition in a community repository (e.g. GitHub). *Nature Methods* guidance for providing algorithms and software for publication provides further information on this topic.

Materials and reagents

Policy information about availability of materials

8. Materials availability

Indicate whether there are restrictions on availability of unique materials or if these materials are only available for distribution by a for-profit company.

No unique materials were used. No restriction on availability of all materials used in this study.

9. Antibodies

Describe the antibodies used and how they were validated for use in the system under study (i.e. assay and species).

NA

10. Eukaryotic cell lines

a. State the source of each eukaryotic cell line used.

NA

b. Describe the method of cell line authentication used.

NA

c. Report whether the cell lines were tested for mycoplasma contamination.

NA

d. If any of the cell lines used are listed in the database of commonly misidentified cell lines maintained by ICLAC, provide a scientific rationale for their use.

NA

Animals and human research participants

Policy information about studies involving animals; when reporting animal research, follow the ARRIVE guidelines

11. Description of research animals

Provide details on animals and/or animal-derived materials used in the study.

NA

Policy information about studies involving human research participants

12. Description of human research participants

Describe the covariate-relevant population characteristics of the human research participants.

NA